Nanoscale Advances

ROYAL SOCIETY OF CHEMISTRY

PAPER

View Article Online
View Journal | View Issue

Cite this: *Nanoscale Adv.*, 2024, **6**, 6420

Injectable pH-responsive polypeptide hydrogels for local delivery of doxorubicin†

Yijun Guo,[a] Yong Chen,[a] Yiqun Wu,[b] Ying Zhu,[b] Shiyao Luo,[b] Juan Shen*[b] and Yongjun Luo*[b]

Cancer, as a global health threat, is often treated with chemotherapy, but its effect is limited, especially the drugs such as doxorubicin (DOX) are limited by their non-specificity and side effects. This study focuses on developing a new drug delivery system to overcome these challenges. Based on the self-assembling peptide hemopressin (HP), we designed and screened FOK peptide, which serves as a pH-responsive carrier with excellent pH sensitivity and mechanical stability. At a concentration of 20 mg mL^{-1}, FOK can spontaneously form a stable hydrogel, efficiently encapsulating DOX with an encapsulation rate exceeding 95%. This system can gradually release the drug in the tumor-specific mildly acidic environment, achieving precise delivery and sustained release of the drug. Rheological analysis revealed the superior mechanical and self-healing properties of FOK hydrogel, suitable for injection delivery with long-lasting stability. Mouse experiments showed that DOX/FOK hydrogel significantly inhibited tumor growth while greatly reducing toxicity. In conclusion, FOK hydrogel, as a delivery vehicle for DOX, not only optimizes the precise delivery and sustained release mechanism of DOX, but also reduces treatment side effects, opening up new avenues for the application of peptide hydrogels in cancer therapy and providing a scientific basis for designing efficient drug delivery systems.

Received 30th August 2024
Accepted 19th October 2024

DOI: 10.1039/d4na00719k

rsc.li/nanoscale-advances

1. Introduction

Cancer, a globally significant public health crisis, continues to cause deep concern due to its high incidence and mortality rates. Particularly, breast cancer, as the most common cancer type among women, has risen to the top of the list of leading causes of female cancer-related deaths worldwide.[1,2] Currently, chemotherapy, as a core and effective clinical strategy for inducing tumor cell apoptosis, faces challenges of low drug targeting delivery efficiency and severe non-specific toxicity to normal cells.[3–5] Doxorubicin (DOX), as a frontline chemotherapy drug in breast cancer treatment,[6,7] is limited in its bioavailability and is associated with multiple adverse reactions such as bone marrow suppression, acute gastrointestinal reactions, and cardiotoxicity,[8,9] significantly limiting its clinical potential.[10,11]

To address this challenge, research on drug delivery systems is flourishing, aiming to enhance the efficacy of anticancer drugs through innovative strategies, optimize drug targeting delivery efficiency, and reduce systemic toxicity to the body. Hydrogels, as a unique physical or chemically cross-linked three-dimensional (3D) network structure,[12,13] have shown promising applications in the biomedical field due to their excellent water swelling properties, biocompatibility, high drug loading capacity, and sustained drug release characteristics. Particularly, hydrogels based on self-assembling peptides, with their rich synthetic diversity, good biocompatibility, flexible modularity, excellent biodegradability, and high drug loading efficiency, have become preferred materials for drug carriers.[14–16] The self-assembly process of peptides is the result of complex interactions and dynamic equilibrium of various non-covalent forces such as internal hydrogen bonding, electrostatic interactions, hydrophobic effects, and π–π stacking, which collectively drive peptide molecules to orderly self-assemble into specific structures.[17,18] By finely tuning the balance of these non-covalent forces, the self-assembly process of peptide molecules can be effectively guided, thereby achieving precise control over peptide structures. Stimuli-responsive delivery systems have become a hot research topic in order to achieve precise enrichment of drugs at tumor sites.[19,20] Based on this, by controlling the driving forces of peptide self-assembly, designing hydrogels with specific stimulus responsiveness provides a new approach for optimizing drug delivery systems.

The tumor microenvironment (TME), as a highly specific and complex ecological system, provides rich inspiration for the

[a]*Department of Pharmacy, Nantong First People's Hospital, Nantong, Jiangsu 226006, China*

[b]*Department of Pharmaceutics, School of Pharmacy, State Key Laboratory of Natural Medicines, China Pharmaceutical University, Nanjing, Jiangsu 211198, China. E-mail: 2385696809@qq.com; 2098717821@qq.com*

† Electronic supplementary information (ESI) available: Mass spectrometry confirmation of peptides, gelation of different concentrations of peptides, gelation of different pH conditions, gelation of peptides with different drug loads, encapsulation efficiency of drug-loading peptide hydrogels and IC_{50} value of DOX and DOX/FOK. See DOI: https://doi.org/10.1039/d4na00719k

design of stimuli-responsive hydrogels due to its unique physiological characteristics such as hypoxia, low pH, high levels of reactive oxygen species, and specific enzyme activities.[21–24] Among them, the acidic microenvironment, as a common and significant feature of solid tumors, with a pH value (6.0–6.5) significantly different from normal tissues (pH $\sim$ 7.4),[25] provides a natural triggering mechanism for the specific release of anticancer drugs at tumor sites. For example, the research team led by Liu[26] designed a pH-responsive peptide hydrogel as a carrier for anticancer drugs such as gemcitabine (GEM) and paclitaxel (PTX). This hydrogel can be locally injected directly into the tumor area and achieve slow and sustained drug release induced by the tumor microenvironment, effectively enhancing the anticancer therapeutic effect. In addition, compared to traditional hydrogel systems, locally injectable hydrogels show broader application prospects. They not only deliver therapeutic drugs precisely to target tissues through simple injection methods, effectively avoiding nonspecific diffusion of drugs to healthy tissues, but also achieve long-term stable drug release, further enhancing therapeutic effects while significantly reducing the incidence of adverse reactions.[27–29]

This study focuses on developing a peptide hydrogel system that integrates pH responsiveness, biocompatibility, and injectability, aiming to utilize the acidic characteristics of the tumor microenvironment to achieve precise local delivery of drug molecules, overcoming the limitations of traditional chemotherapeutic drugs such as doxorubicin (DOX) in treating tumors. Based on the molecular design of hemopressin (HP), we used a solid-phase synthesis strategy to carefully synthesize four self-assembling peptides (POH, POK, FOH, FOK), among which the FOK peptide not only exhibits excellent pH sensitivity but also possesses outstanding mechanical strength and structural stability. This innovative peptide can form a stable drug-loaded peptide hydrogel (DOX/FOK) under physiological pH conditions, which can be precisely located at the tumor site through injection. Under the acidic stimulation of the tumor microenvironment, this hydrogel can gradually degrade, achieving slow drug release, thereby enhancing the anti-tumor effect while significantly reducing the toxic side effects of the drug on normal tissues. Therefore, this pH-responsive peptide hydrogel system shows broad clinical application prospects, opening up new avenues for cancer treatment and laying a solid foundation for the future development of drug delivery systems.

2. Materials and experiments

2.1 Materials

Fmoc-protected amino acids, Wang resin, *N*,*N*-diisopropylcarbodiimide (DIC), 1-hydroxybenzotriazole (HOBT), and acetic anhydride were purchased from Shanghai J&K Scientific Ltd (Shanghai, China). EDT was bought from Shanghai BOC Sciences Co., Ltd (Shanghai, China). Triisopropylsilane (TIS) was purchased from Suzhou Crystal Clear Chemical Co., Ltd (Suzhou, China). Pyridine was purchased from Shanghai Lingfeng Chemical Reagent Co., Ltd (Shanghai, China). Chromatography-grade acetonitrile was purchased from MERCK (Germany). Mass spectrometry-grade formic acid and chromatography-grade trifluoroacetic acid (TFA) were purchased from Bailingwei Technology Co., Ltd (Beijing China). Ultrapure water was bought from Hangzhou Wahaha Group Co., Ltd (Hangzhou, China). Hydrochloric acid, sodium chloride, sodium hydroxide, methanol, dichloromethane (DCM), dimethyl sulfoxide (DMSO) and *N*,*N*-dimethylformamide (DMF) were bought from Nanjing Chemical Reagent Co., Ltd (Nanjing, China). Ether, hemopressin (HP), cell-permeable near-infrared fluorescent probe DiR and doxorubicin (DOX) were purchased from Shanghai Aladdin Bio-Chem Technology Co., Ltd (Shanghai, China). Mouse breast cancer cells (4T1 cells), DMEM culture medium and Cell Counting Kit-8 (CCK-8) were purchased from Jiangsu KeyGen Biotech Co., Ltd (Jiangsu, China). Other reagents were analytical grade and used as received.

2.2 Experiments

2.2.1 Design of peptides. Hemopressin (HP), a nine-peptide derived from the alpha chain of hemoglobin (PVNFKFLSH; Pro1-Val2-Asn3-Phe4-Lys5-Phe6-Leu7-Ser8-His9), can self-assemble into reverse parallel β fiber hydrogels under physiological conditions,[30–32] but it has weaknesses such as poor mechanical properties and low pH sensitivity. The self-assembly of HP is mainly driven by the attractive forces between the π–π stacking of two phenylalanine residues at positions 4 and 5 and the intermolecular hydrogen bonds between adjacent peptide amides.[33] To overcome these limitations, we carefully designed four modified peptides aimed at imparting stronger pH responsiveness and optimized mechanical properties to achieve slow drug release function induced by the tumor microenvironment. Specifically, our design strategy is as follows:

(1) Enhancing pH sensitivity: substituting the lysine (Lys, K, PI = 9.74) at the fifth position of HP with ornithine (Orn, O, PI = 10.80) with a higher isoelectric point. Under weak acidic conditions, ornithine side chains are more prone to protonation, thereby enhancing the sensitivity of the entire peptide chain to pH changes.

(2) Improving mechanical strength: considering the non-polar and hydrophobic characteristics of phenylalanine (Phe, F) and its ability to promote beta-fold formation, we replaced the proline (Pro, P) at the head with phenylalanine. This adjustment aims to enhance the beta-fold tendency of the sequence to improve the mechanical stability of the peptide hydrogel.

(3) Enhancing solubility and pH sensitivity: substituting histidine (His, H) at the tail with lysine (Lys, K), lysine is a polar amino acid with a higher isoelectric point than histidine, which can increase the solubility of the peptide in water. Through the protonation–deprotonation process of its side chain, lysine may further amplify the pH responsiveness of the peptide and enhance its pH sensitivity.

Based on the above design principles, we constructed four novel peptides and named them based on the positions of the substituted amino acids: POH (only replacing Lys with Orn), POK (replacing Lys with Orn and His with Lys), FOH (replacing Lys with Orn and Pro with Phe), and FOK (replacing Pro at the

head, Lys in the middle, and His at the tail with Phe, Orn, and Lys).

2.2.2 Peptide synthesis, purification, and characterization. Using the Fmoc protection group strategy and Wang resin, peptides were synthesized in solid phase. 1.5 g of Wang resin (substitution degree 0.32 mmol g^{-1}) was pre-swollen in 7 mL of DCM and washed three times. The C-terminal starting amino acid (1.5 mmol) and HOBt (1.5 mmol) were dissolved in DCM, followed by the addition of DIC (1.5 mmol) as the coupling agent. The initial coupling reaction was completed after 4 hours. Subsequently, 5 mL of 20% acetic anhydride was added for an additional 1 hour of reaction to cap any unreacted groups and prevent the formation of by-products. After the reaction, the resin was filtered, washed, and set aside. A solution of 5 mL of DMF containing 20% piperidine was added to remove the Fmoc protection group, followed by three washes. This cycle was repeated for each amino acid addition, and the success of each coupling step was confirmed by bromophenol blue testing. Finally, peptides were cleaved using 5 mL of cleavage solution (TFA : TIS : water = 95 : 3 : 2). After 3 hours of cleavage, the crude product was precipitated with ether and centrifuged at low temperature. Purification of the products was carried out using an LC-8A Shimadzu high-performance liquid chromatography system with a C18 reverse-phase column (340 mm × 28 mm, 5 μm) and a mobile phase of 0.1% TFA aqueous solution and 0.1% TFA acetonitrile solution. Characterization of all peptides was performed using an ACQUITY liquid chromatography-mass spectrometry system (WATERS, USA) to confirm purity and molecular weight.

2.2.3 Performance evaluation and optimization of peptide hydrogels

2.2.3.1 Self-assembly concentration of peptide hydrogels study. To systematically investigate the effect of peptide concentration on the self-assembly properties of peptide hydrogels, this study designed four sets of experiments for FOK, FOH, POK, and POH peptides. Different doses (1.5, 2.0, 2.5, 3.0 mg) of each peptide were weighed into 1.5 mL EP tubes and dissolved in NaCl solution (100 μL, 150 mM) to prepare peptide solutions of different concentrations (15, 20, 25, 30 mg mL^{-1}). Subsequently, by adjusting NaOH (0.1 M) to pH 7.4, the solutions were left at ambient conditions to observe and record the transition from solution state to gel state, aiming to identify the peptides most suitable for self-assembly and their concentration range.

2.2.3.2 pH-dependent self-assembly behavior study. To investigate the effect of pH changes on the formation ability of peptide hydrogels, each peptide (2.0 mg) was dissolved in NaCl solution (100 μL, 150 mM) to prepare solutions with an initial concentration of 20 mg mL^{-1}. Subsequently, the pH value was adjusted using NaOH/HCl (0.1 M) solutions to systematically examine the morphological changes of peptide solutions under different pH conditions, with a focus on the assembly stability and responsiveness in weakly acidic and neutral environments, providing a theoretical basis for subsequent drug delivery strategies.

2.2.3.3 Research on the drug loading capacity of peptide hydrogel. The encapsulation of DOX by FOX hydrogel primarily utilizes a physical embedding method, leveraging the hydrophobic interaction between the drug and the hydrophobic core of the hydrogel to encapsulate the drug within the hydrogel.[34,35] To evaluate the drug-loading capacity of four peptides as drug carriers, 5 mg of DOX was first dissolved in NaCl solution (100 μL, 150 mM) to prepare a stock solution (50 mg mL^{-1}). Subsequently, under the condition of fixed peptide concentration at 20 mg mL^{-1}, a series of peptide solutions with drug concentrations of 1, 2, and 3 mg mL^{-1} were prepared by gradually adding different volumes of the DOX stock solution and adjusting to pH 7.4. The changes in solution state were carefully observed and recorded to examine the loading efficiency and stability of the peptides towards the drug.

2.2.3.4 Study on the release behavior of drug-loaded peptide hydrogels in vitro. This study further investigated the drug release behavior of four peptides in simulated physiological (pH 7.4) and tumor microenvironment (pH 6.0). 2.0 mg of peptide and DOX (2 μL, 50 mg mL^{-1}) were co-dissolved in NaCl solution (98 μL, 150 mM) to form a drug concentration of 1 mg per mL solution, and adjusted to the desired pH value, then allowed to stand to form a stable hydrogel. Subsequently, the gel was exposed to PBS buffer at different pH values and continuously incubated in a constant temperature shaker (37 °C, 120 rpm min^{-1}) for 7 days. At different time points (1, 3, 6, 9, 12, 24, 48, 72, 96, 120, 144, 168 h), all release media were collected and replaced with the same volume of fresh release media. The release amount of DOX was monitored using UV spectrophotometry, cumulative release curves were plotted to analyze the release kinetics of each peptide carrier.

2.2.3.5 Investigation of the effect of peptide concentration on the in vitro release behavior of drug-loaded hydrogels. The effect of different concentrations (20, 25, 30 mg mL^{-1}) of FOK polypeptide on the drug release behavior of drug-loaded hydrogels (DOX/FOX) was investigated. By preparing DOX/FOX with a fixed DOX concentration (1 mg mL^{-1}) but varying polypeptide concentrations, *in vitro* release experiments were conducted under identical conditions to examine the influence of different polypeptide concentrations on the drug release behavior of the drug-loaded hydrogels. The optimal polypeptide concentration was selected to optimize the drug delivery system.

2.2.3.6 The influence of drug concentration on the in vitro release behavior of polypeptide hydrogels. In addition, this study also extensively investigated the influence of drug concentration (1, 2, 3 mg mL^{-1}) on the release behavior of drug-loaded hydrogels (DOX/FOX). Under the condition of fixed peptide concentration (20 mg mL^{-1}), hydrogels with different drug loading concentrations were prepared by changing the loading amount of DOX, and their release characteristics were systematically analyzed to determine the most suitable drug concentration.

2.2.4 FOX representation and pH responsiveness. Weigh 8.0 mg of FOK into a sample vial, add 400 μL of NaCl solution (150 mM), and vortex thoroughly to obtain a 20 mg per mL FOX polypeptide solution. Subsequently, to investigate the effect of pH on the properties of FOK, we adjusted the pH of the peptide solution to 7.4 and 6.0 using 0.1 M NaOH/HCl solution, and photographed the gel and solution forms in a tilted state. Dynamic light scattering (DLS) technique was employed to

examine the particle size distribution and zeta potential of FOK nanofibers under different pH conditions. Samples were dropped onto a carbon-coated copper grid, and transmission electron microscopy (TEM) was used to observe the microstructure of FOK hydrogels under different pH conditions. Circular dichroism (CD) spectroscopy was utilized to determine the structural changes of FOK under different pH conditions, recording the CD spectra in the wavelength range of 190–250 nm at a scanning speed of 50 nm min^{-1}.

2.2.5 Characterization of DOX peptide hydrogel (DOX/FOX). FOH and FOK were each weighed at 8.0 mg in the sample vial, followed by the addition of NaCl solution (492 μL, 150 mM), and then the addition of DOX stock solution (2 mg mL^{-1}, 8 μL). The mixture was thoroughly vortexed to obtain the DOX/FOX hydrogel. The pH was adjusted to 7.4 using 0.1 M NaOH/HCl solution, and the hydrogel was allowed to gel by standing still. The morphological characteristics of the peptide gel in a tilted state were photographed. The microstructure of the DOX/FOK hydrogel was examined using transmission electron microscopy (TEM). To evaluate the encapsulation efficiency of the peptide hydrogel, DOX/FOX hydrogels containing different concentrations of DOX (1, 2, 3 mg mL^{-1}) were prepared. The pH was adjusted to 7.4, and after the formation of stable drug-loaded gels, the gel surface was washed three times with pH 7.4 PBS. The wash solution was collected for analysis to calculate the amount of DOX not encapsulated in the hydrogel, thereby determining the encapsulation rate of the drug gel. The calculation formula is as follows: Encapsulation rate (%) = [(initial amount of DOX − amount of DOX in wash solution)/initial amount of DOX] × 100%.

2.2.6 Rheology test. The rheological properties of the hydrogels were systematically studied using a rheometer (HAAKE 6000, Thermo Fisher Scientific, USA). The hydrogels were placed between parallel plates with a diameter of 8 mm and a gap of 0.5 mm under oscillatory mode at 37 °C. The storage modulus (G') and loss modulus (G'') of FOX hydrogel and DOX/FOX hydrogel were evaluated through frequency scans ranging from 1 to 100 rad s^{-1}. Strain scans were set from 0.1% to 100% at a frequency of 6.28 rad s^{-1}. To observe the self-healing ability of the hydrogels, continuous step strain tests were conducted with strains ranging from 1% to 50% at a frequency of 6.28 rad s^{-1}, which is crucial for the injectability of the hydrogels.

2.2.7 Stability assessment. Long-term experiments are an important basis for assessing the stability of formulations. FOK and DOX/FOK were placed under the conditions of 25 °C ± 2 °C and relative humidity of 60% ± 5% for 6 months to observe their appearance and conduct cyclic strain time scanning experiments.

2.2.8 *In vitro* cytotoxicity study. The cytotoxicity experiment was conducted using the Cell Counting Kit-8 (CCK-8) assay. 4T1 cells were uniformly seeded in a 96-well plate at a predetermined density (5×10^4 cells per mL) and incubated for 24 hours in a constant temperature incubator (5% CO_2, 37 °C). Subsequently, the release fluid of DOX/FOK hydrogel under pH 6.0 and pH 7.4 conditions after 48 hours of release was collected separately. The release fluid at different pH values and DOX solutions (0.1, 1, 10, 50 μg mL^{-1}) were added to the 96-well plate and incubated at 37 °C for 24 hours, with the same volume of DMEM culture medium used as a blank control. After incubation, 10 μL of CCK-8 reagent was added to each well and further incubated for 4 hours in the incubator. The absorbance (OD) value of each well at 450 nm was then measured using a microplate reader to evaluate cell viability. Each sample was tested in quintuplicate ($n = 5$) and the results were reported as mean ± SD. Additionally, to comprehensively assess the potential toxicity of FOK blank hydrogel on 4T1 cells, we conducted experiments with different concentrations (1, 10, 50, 100, 200, 400 μg mL^{-1}) of FOK blank hydrogel following the same experimental procedure.

2.2.9 *In vivo* anti-tumor research. The female BALB/c mice (6 weeks old, 16–18 g) used in the experiment were sourced from the Experimental Animal Center of China Pharmaceutical University. All animal procedures were performed in accordance with the Guidelines for Care and Use of Laboratory Animals of China Pharmaceutical University and approved by the Animal Ethics Committee of China Pharmaceutical University (Ethical Number: 2024-10-096). The mice were acclimated for one week in a specific environment.

To establish a mouse model of breast cancer, 4T1 cell suspension (1×10^7 cells per mL, 100 μL) was inoculated subcutaneously into the right forelimb axilla of healthy mice. After inoculation, the mice were kept in standard observation rooms and their growth was monitored. The weight and tumor volume of the mice were recorded daily. When the tumor volume reached approximately 100 mm^3, 15 mice were randomly divided into 3 groups ($n = 5$): normal saline control group (NS group), DOX group (1 mg mL^{-1}), and DOX/FOX group (dose ratio 1 mg mL^{-1} : 20 mg mL^{-1}). Samples (100 μL/20 g) were administered near the tumor tissue by subcutaneous injection, ensuring that each mouse received a dose of 10 mg of doxorubicin per kilogram of body weight. The day of administration was considered as day 1, and the weight and tumor volume of the tumor-bearing mice were recorded. After 7 days of administration, all experimental mice were euthanized, and the hearts, livers, spleens, lungs, kidneys, and tumors of the mice were collected, fixed in 10% formalin, and subjected to H&E staining and Tunel detection analysis. The formula for calculating tumor volume (V) is as follows: $V = L \times W2/2$ where L is the long diameter of the tumor and W is the short diameter of the tumor.

2.2.10 *In vivo* biological distribution analysis. The *in vivo* biological distribution of the hydrogel was analyzed using the near-infrared fluorescent dye DiR. As described above, 4T1 tumor-bearing mice (with tumor volume of approximately 200 mm^3) were randomly divided into 2 groups ($n = 3$): the DiR group (1 mg kg^{-1}) and the DiR/FOK group (equivalent dose of 1 mg per kg DiR). The drugs were subcutaneously injected near the tumor (100 μL/20 g). The mice were then anesthetized, and live imaging analysis of the tumor-bearing mice was performed at predetermined time points (1, 6, 12, 24, 48, and 96 hours) (λ_{ex} = 748 nm, λ_{em} = 780 nm). After 96 hours, the mice were euthanized, and the heart, liver, spleen, lungs, kidneys, and

tumor tissues were collected for *ex vivo* biological distribution analysis.

2.2.11 *In vivo* biocompatibility study. To investigate the *in vivo* biocompatibility of FOK blank hydrogel, we carefully selected 6 female BALB/c mice with similar body weights and good health status as experimental subjects. They were randomly divided into two groups, with 3 mice in each group, and injected with 100 μL of normal saline and 100 μL of FOK blank hydrogel subcutaneously on the back of the mice. Three days later, the mice were euthanized, and the subcutaneous tissues around the injection site were dissected for H&E staining to observe inflammatory reactions.

2.2.12 Statistical analysis. Quantitative data were presented as means ± SD. One-way ANOVA was used to assess statistical differences among three or more groups.

3. Results and discussion

3.1 Design and synthesis of peptides

In this project, we carefully designed four peptide sequences with pH-responsive properties, named POH, POK, FOH, and

Table 1 Sequence of the designed peptides

Peptide	Sequence
PVNFOFLSH (POH)	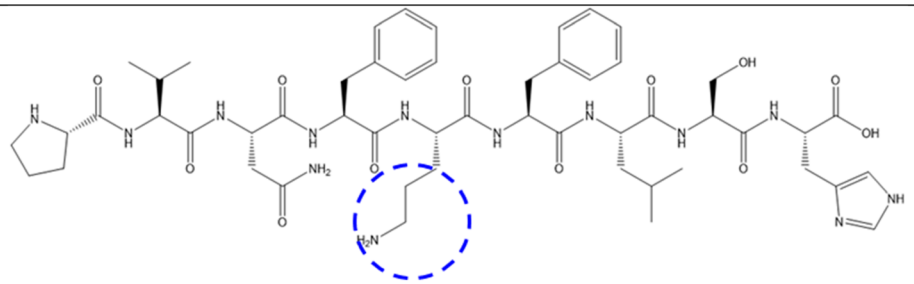
PVNFOFLSK (POK)	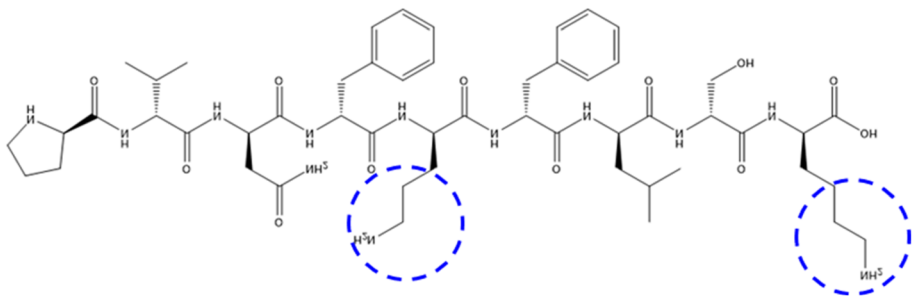
FVNFOFLSH (FOH)	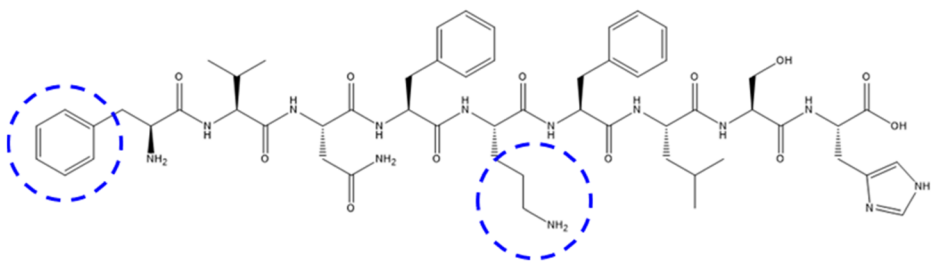
FVNFOFLSK (FOK)	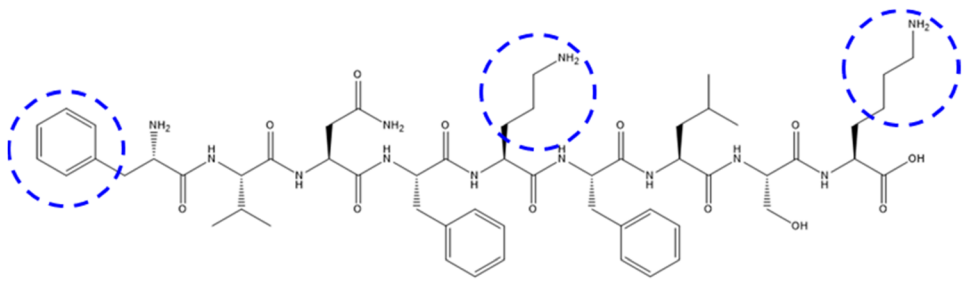

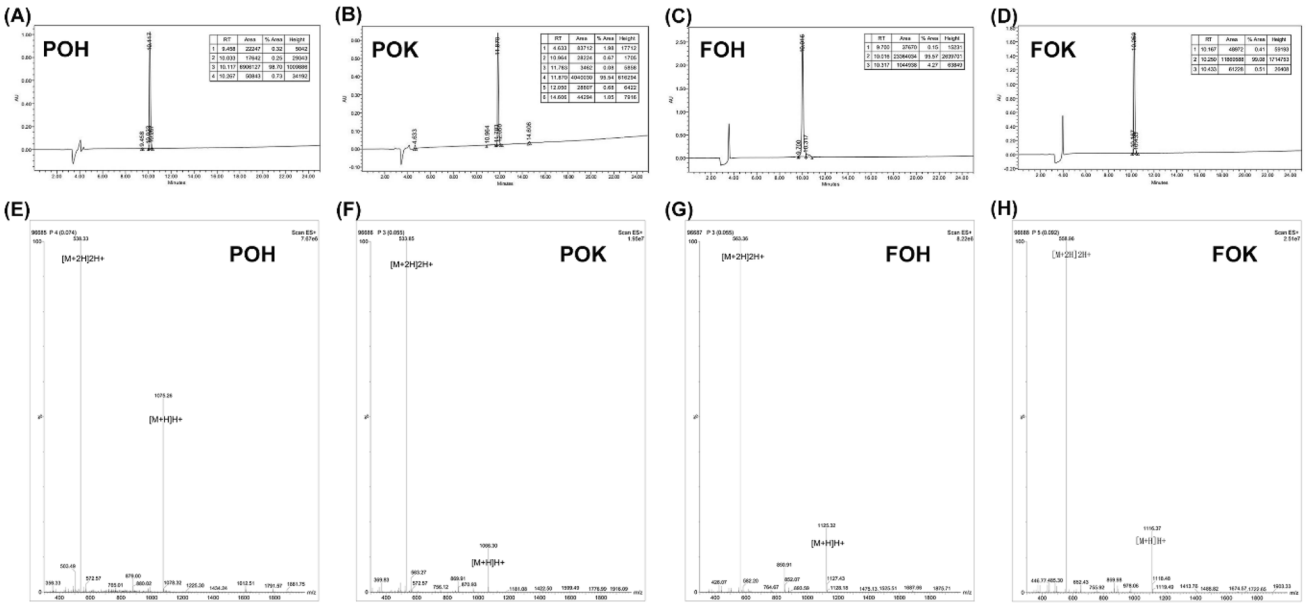

Fig. 1 HPLC chromatogram of (A) POH, (B) POK, (C) FOH and (D) FOK. Mass spectrum of peptides (E) POH, (F) POK, (G) FOH and (H) FOK.

FOK, as shown in Table 1. These peptides were strategically modified based on the HP prototype. In POH, the fifth position was replaced with the basic amino acid Orn to enhance its pH-responsive ability. In POK, the fifth and ninth positions were replaced with Orn and the hydrophilic amino acid Lys, aiming to enhance both pH sensitivity and water solubility. In FOH, the first and fifth positions were replaced with the hydrophobic amino acid Phe and Orn to improve mechanical strength and pH sensitivity. In FOK, the first, fifth, and ninth positions were replaced with Phe, Orn, and Lys, respectively, to comprehensively enhance the mechanical strength, pH sensitivity, and water solubility of the peptides. All four peptides were synthesized using solid-phase synthesis with Wang resin as the carrier, coupled from the C-terminus to the N-terminus. After purification by reverse-phase high-performance liquid chromatography (RP-HPLC), the purity and molecular weight of the peptides were analyzed using high-performance liquid chromatography-mass spectrometry (HPLC-MS). The purity of POH, POK, FOH, and FOK was found to be 98.70%, 95.54%, 95.57%, and 99.08% (Fig. 1A–D), respectively, meeting the purity requirements for subsequent peptide preparation and evaluation. The mass spectrometry analysis of each peptide is shown in Table S1.† The theoretical values of the multi-charged peaks calculated from the peptides were highly consistent with the detected values (Fig. 1E–H), confirming that the purified nonapeptide sequences fully matched the expected design and maintained a high level of purity above 95%, meeting the requirements of scientific research design and experimentation.

3.2 Screening and optimization of peptides

This study investigated the gelation properties of four peptides (POH, POK, FOH, FOK) and their potential as drug carriers. The results (Table S2†) showed that POH and POK were unable to form stable hydrogels in the concentration range of 15 to 30 mg mL^{-1}, attributed to the high protonation of Orn at position 5, weakening the hydrophobic interactions between Phe at positions 4 and 6, thereby hindering the effective formation of β-folded nanofibers and weakening the gelation performance. In contrast, FOH and FOK could both form stable peptide hydrogels at concentrations of 20 mg mL^{-1} and above, with the gelation speed increasing with concentration. This was attributed to the substitution of Pro at the head by Phe with a stronger β-folding tendency, enhancing the self-assembly efficiency and rate of the peptides. Under pH 7.4 conditions, FOH and FOK could both form stable hydrogels (Table S3†), benefiting from the π–π stacking and hydrophobic interactions of the Phe aromatic residues promoting self-assembly. However, under acidic conditions at pH 5.5, they remained in solution state due to the dominance of electrostatic repulsion, hindering fiber elongation and self-assembly process, leading to gel disintegration. It is worth noting that FOH exhibited a transiently unstable gel state at pH 6.0 in a slightly acidic environment, while FOK remained a viscous solution, indicating that the replacement of His with Lys enhanced the pH sensitivity of the peptides.

The drug loading experiment (Table S4†) showed that after loading with POH and POK, stable hydrogels could not be formed, while FOH and FOK could both form stable drug-loaded hydrogels after loading 1–3 mg per mL DOX, meeting the requirements for anti-tumor drug delivery. Further analysis (Fig. 2A) revealed that the cumulative drug release of FOH and FOK under pH 6.0 conditions (59.21%, 68.73%) was significantly higher than at pH 7.4, especially for FOK, whose release in acidic environments was 3.03 times that in neutral conditions, demonstrating excellent responsiveness to the tumor microenvironment and thus selected as the focus of optimization studies.

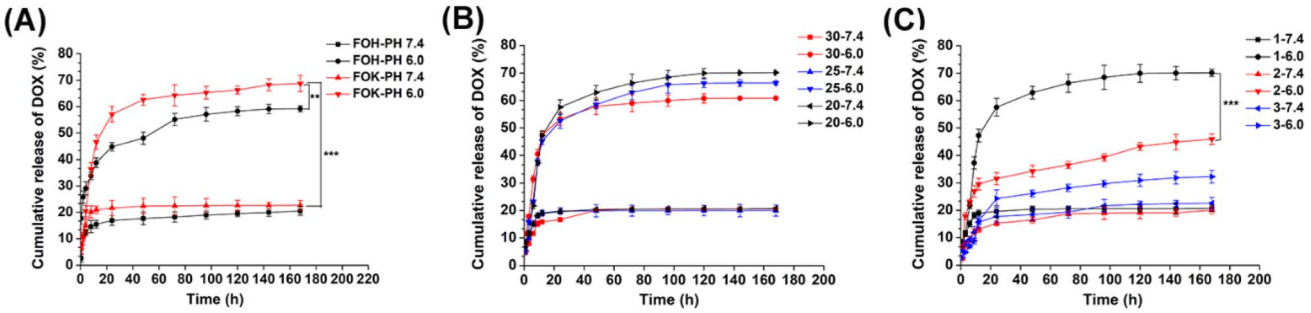

Fig. 2 (A) Cumulative release of DOX from hydrogel FOK and FOH in different buffer solution. (B) Cumulative release of DOX from hydrogel FOK with different peptide concentration. (C) Cumulative release of DOX from hydrogel FOK with different DOX concentration. $^{**}P < 0.01$, $^{***}P < 0.001$.

Based on the evaluation of different concentrations (20, 25, 30 mg mL^{-1}) of drug release for FOK (Fig. 2B), it was observed that at a fixed DOX concentration (1 mg mL^{-1}), the drug release in pH 7.4 environment was around 20% for all concentrations. However, at pH 6.0, as the concentration of FOX increased, the drug release decreased from 70.19% to 60.83%. This phenomenon indicates that the dense fiber network formed by high concentration peptides has a hindering effect on drug release. Considering drug utilization, chemotherapy effectiveness, and synthesis cost, we determined 20 mg mL^{-1} as the optimal gel concentration for FOK to achieve the best drug delivery effect at the tumor site.

The *in vitro* release of 1–3 mg per mL DOX by FOX hydrogel was explored (Fig. 2C), and it was found that the release rate decreased as the DOX concentration increased. This phenomenon was attributed to the increased number of drug molecules within the polypeptide hydrogel, which enhances their intermolecular interactions and concurrently occupies a significant portion of the gel network's space, resulting in narrowed or even blocked diffusion channels, and subsequently decreased release rates.[36,37] Under pH 6.0 conditions, 1 mg per mL DOX exhibited the best release performance, with an accumulated release of 69.5% in 7 days, significantly higher than 2 mg mL^{-1} (44.6%) and 3 mg mL^{-1} (32.3%). Therefore, 1 mg mL^{-1} was selected as the optimal drug loading concentration to optimize drug delivery efficiency.

3.3 FOX hydrogel characterization and pH responsiveness

According to Fig. 3A, it can be seen that FOK forms a stable hydrogel at a concentration of 20 mg mL^{-1} in a pH 7.4 environment, exhibiting semi-solid characteristics and maintaining stable morphology when tilted. At pH 6.0, it transforms into a highly viscous liquid, indicating significant pH sensitivity and suggesting its potential as a carrier for anti-tumor drugs. Transmission electron microscopy (TEM) (Fig. 3B and C) revealed the microstructural differences of FOK at different pH levels: at pH 7.4, it formed a dense interwoven nanofiber network, providing space for drug loading; at pH 6.0, it appeared as short and dispersed peptide forms, with the nanofiber network disappearing, directly confirming its pH-responsive characteristics. Particle size and zeta potential analysis (Fig. 3D–F) further elucidated these changes. At pH 7.4, the fiber size was concentrated in the range of 1900–2000 nm, with a low charge (5.41 ± 0.78 mV), indicating that attraction between oppositely charged amino acid residues promoted the self-assembly of nanofibers; at pH 6.0, the size decreased to 600–900 nm, with a significant increase in positive charge (17.88 ± 1.28 mV), attributed to protonation of basic amino acids enhancing charge repulsion, leading to nanofiber disassembly. Circular dichroism analysis (Fig. 3G) revealed the dynamic process of FOK peptide secondary structure changes with pH variation. At pH 7.4, characteristic peaks of β-folded configuration were observed, indicating that peptides were predominantly in a β-folded state; while at pH 6.0, the spectrum shifted to features of irregularly coiled conformations, suggesting that the acidic environment induced structural rearrangement of peptides. Based on this, it is speculated that as the pH increases from 6.0 to 7.4, the peptide structure transitions from irregular coiled conformations to a coexistence of β-folding and irregular coiling, indicating the gradual transformation of peptides from a solution state to a fiber network and eventually forming a hydrogel.

3.4 DOX/FOX representation

At concentrations of 20 mg mL^{-1} for FOX and 1 mg mL^{-1} for DOX, FOK and DOX/FOK hydrogels stably formed, exhibiting a semi-solid state characteristic, even when the vial was tilted, they did not flow or disperse (Fig. 3H). Under pH 7.4 conditions, TEM images (Fig. 3I) showed that the microstructure of FOK remained unchanged before and after drug loading, confirming the feasibility of FOK as a carrier for DOX. Furthermore, the encapsulation efficiency data (Table S5†) indicated that with increasing DOX concentration, the encapsulation efficiency of FOX gradually decreased but remained at a high level of over 95%, demonstrating the outstanding drug loading efficiency and high drug content of FOK, indicating its potential as a highly effective drug delivery system.

3.5 Rheology test

Rheological properties, as an important parameter of hydrogels, profoundly affect their efficacy as drug carriers.[38] Dynamic strain scan results show (Fig. 4A) that the critical strain values of

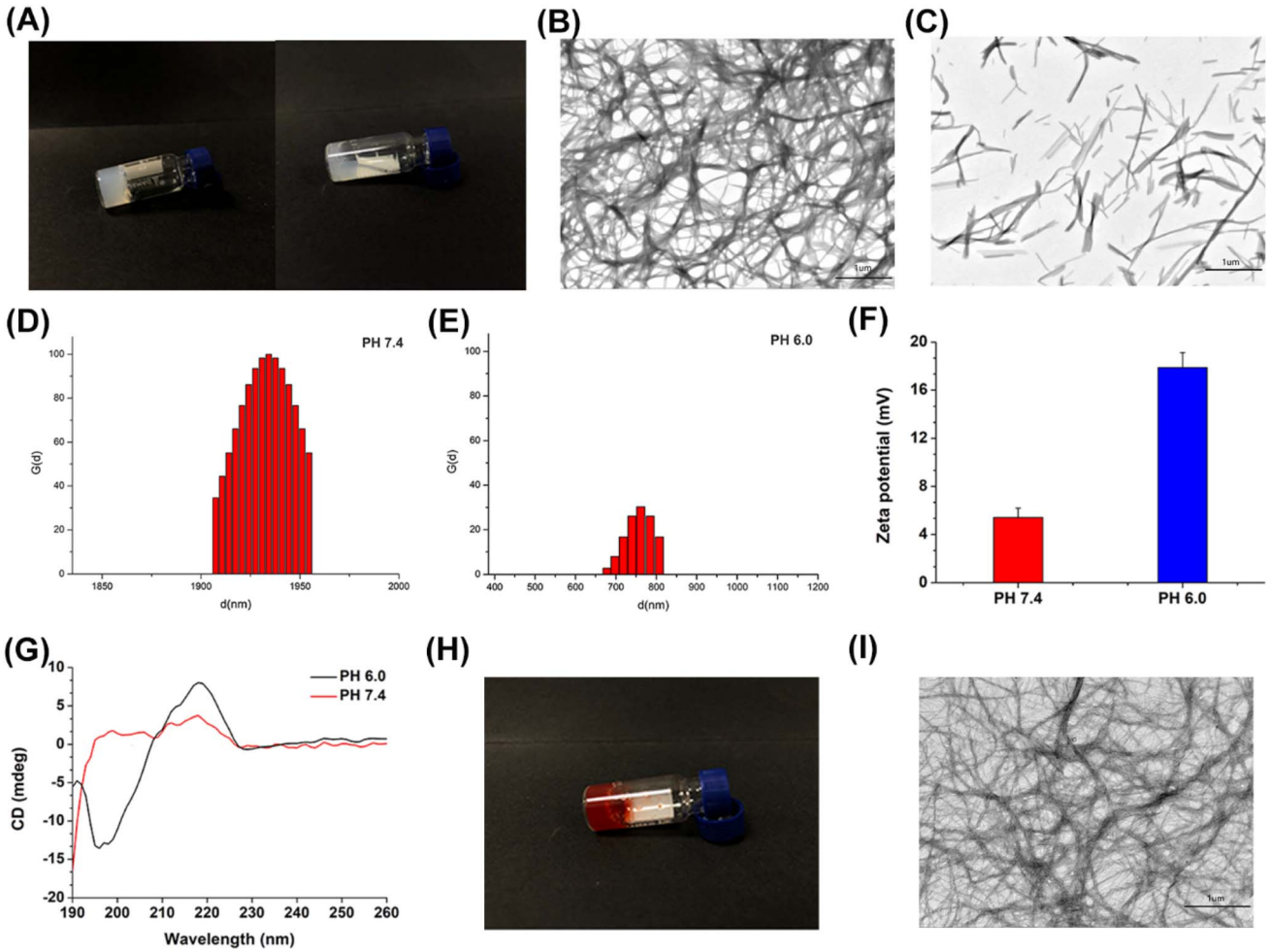

Fig. 3 (A) Appearance of FOK (right) peptide hydrogels at pH 6.0 and FOK (left) peptide hydrogels at pH 7.4. Transmission electron microscopy of 0.20 wt% FOK at (B) pH 7.4 and (C) pH 6.0. DLS curves of FOK hydrogel in (D) pH 7.4 and (E) pH 6.0. (F) zeta potential curves of FOK hydrogel in different buffer ($n = 3$). (G) Circular dichroism spectrum of FOK in different buffer. (H) Appearance of DOX/FOK peptide hydrogels under neutral conditions. (I) Transmission electron microscopy of 0.20 wt% DOX/FOK at pH 7.4.

FOK and DOX/FOK are 11.74% and 9.27%, respectively. Before the critical point, both remain in a solid stable state, but transition to a liquid state after this point, revealing their resistance to external forces. However, the mechanical strength of DOX/FOK decreases after drug loading, attributed to the synergistic effect of DOX's hydrophilicity and the high hydrophilicity of FOK peptides, enhancing the hydrophilicity of the drug delivery system and weakening the interactions between hydrophobic amino acids, which is the main driving force for hydrogel self-assembly.[39] This finding emphasizes the importance of controlling the concentration of DOX to maintain the integrity of the hydrogel structure, consistent with previous studies on drug concentration. Dynamic frequency scans further confirm (Fig. 4B) that within the frequency range of 0.1–10 Hz, the G' and G'' of FOK and DOX/FOK show no significant changes, with G' greater than G'', indicating a stable gel state. Although the drug slightly reduces the mechanical strength, overall stability is maintained, consistent with the strain scan results. In the cyclic strain time scan simulating the injection process (Fig. 4C and D), FOK and DOX/FOK hydrogels exhibit significant self-healing properties. Under high strain (50%), deformation and flow occur, while under low strain (1%), they quickly return to a solid-like state ($G' > G''$), demonstrating the ability to resist external forces. This characteristic not only meets the requirements of injectable drug delivery but also avoids the need for surgical implantation, potentially enhancing patient treatment experience and compliance.

3.6 Stability study

This study conducted a six-month stability evaluation on the optimized FOX and DOX/FOX hydrogels to ensure their stability and effectiveness throughout their shelf life. The results showed (Fig. 5A) that both hydrogels maintained their gel form with no signs of flow and no change in appearance after long-term storage. Through cyclic strain-time sweep analysis (Fig. 5B and C), the FOK and DOX/FOK hydrogels exhibited a certain degree of self-healing properties, and after being left to stand for six months, both their G' and G'' increased to varying degrees compared to their previous states, indicating that FOK

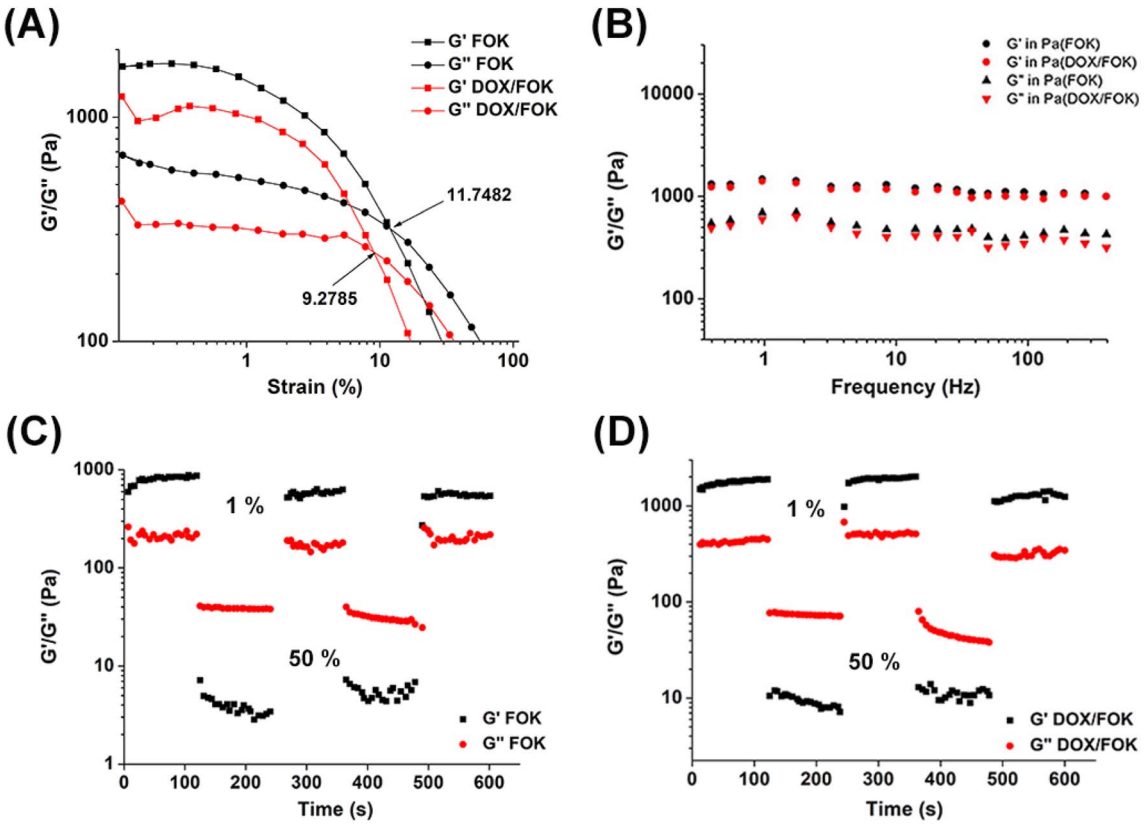

Fig. 4 (A) Dynamic strain sweep of FOK and DOX/FOK hydrogels. (B) Dynamic frequency scanning of FOK and DOX/FOK hydrogels. Circle sweep of (C) FOK and (D) DOX/FOK hydrogels.

and DOX/FOK retained their injectability while enhancing their mechanical properties. In summary, the FOK and DOX/FOK polypeptide hydrogels exhibit good stability and can be stored and applied for a long time.

3.7 *In vivo* anti-tumor research

Fifteen tumor-bearing mice were randomly divided into three groups ($n = 5$) and given NS, free DOX (1 mg mL^{-1}), and DOX/FOX hydrogel (1 mg mL^{-1} : 20 mg mL^{-1}) to evaluate the effects of different administration methods on mouse body weight, tumor growth, and tissue histology. As shown in the figures (Fig. 6A and B), the body weight of mice in the free DOX group significantly decreased (from 18.8 g to 16.9 g within 7 days), indicating the strong toxic side effects of DOX. In contrast, mice in the NS and DOX/FOX hydrogel groups showed an increase in body weight, suggesting that the DOX/FOX hydrogel system effectively alleviated the toxic side effects of DOX. In terms of tumor growth inhibition (Fig. 6C and D), the tumor volume in the NS group increased sharply (reaching 762.42 mm^3 within 7 days), while both the DOX and DOX/FOX groups exhibited significant tumor growth inhibition. However, starting from day 4, the tumor growth in the DOX group accelerated, possibly due to rapid consumption and inadequate retention of DOX at the tumor site. In contrast, the tumor in the DOX/FOX group remained stable, forming a "drug reservoir" at the tumor site for sustained drug release under the stimulation of the tumor microenvironment. At the end of the treatment, the tumor volume in the DOX/FOX group (reduced from 109.65 mm^3 to 81.50 mm^3) was significantly smaller than that in the NS and free DOX groups. These results highlight the effective tumor cell inhibition, continuous slow drug release, prolonged drug action time, and reduced toxicity advantages of DOX/FOX. Further histopathological analysis (Fig. 6E) revealed no obvious apoptotic cells, inflammatory cell infiltration, or local bleeding in the tumor tissue of the NS group, while significant necrotic areas, sparse cell arrangement, dissolved and deformed cell nuclei were observed in the DOX and DOX/FOX groups, with a larger necrotic area in the DOX/FOX group. Tunel detection further confirmed that the DOX/FOX group had the highest number of apoptotic tumor cells, with strong green fluorescence signals, indicating excellent anti-tumor activity and apoptosis induction ability of this hydrogel system. In conclusion, the FOX peptide hydrogel, as a drug carrier, not only achieved controlled release and reduced toxicity of DOX but also significantly enhanced the anti-tumor effect, providing a novel and efficient strategy for cancer treatment.

3.8 *In vivo* distribution study

To investigate the distribution of drug-loaded hydrogel in mice, DiR fluorescent dye was used instead of anti-tumor drugs encapsulated in FOX hydrogel, and its dynamic distribution in tumor-bearing mice was monitored using *in vivo* imaging

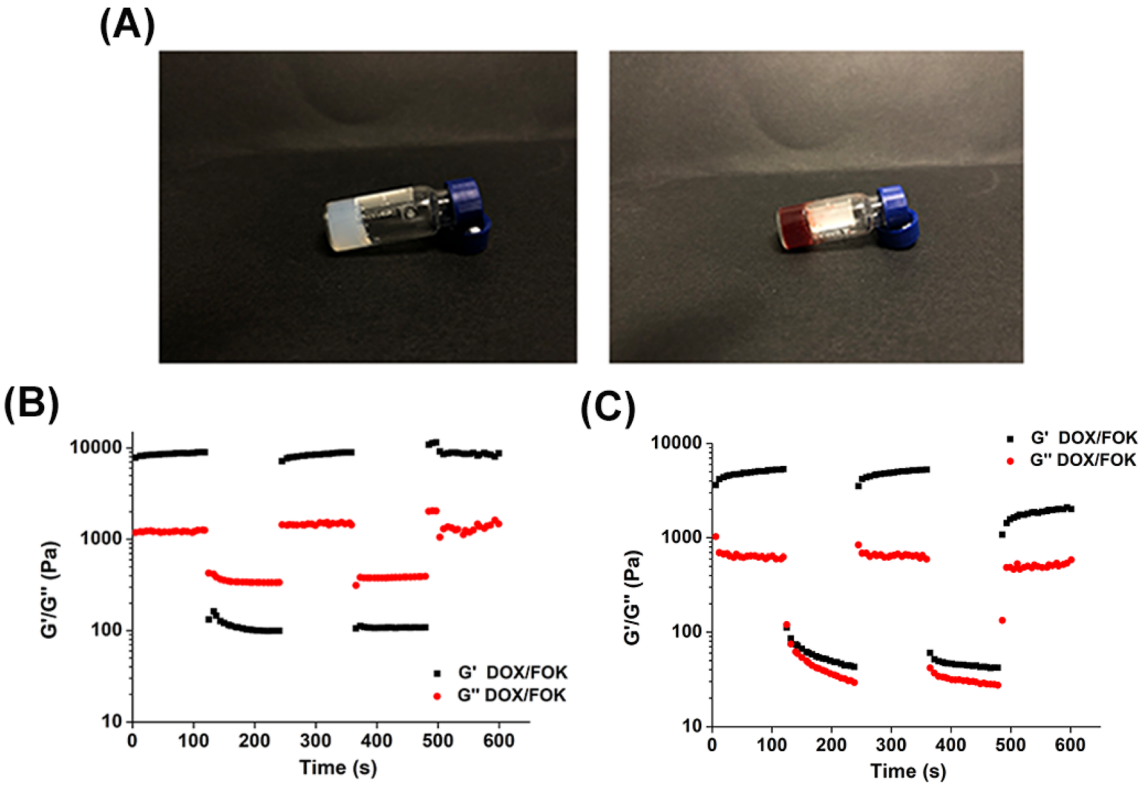

Fig. 5 (A) Appearance of FOK (left) peptide hydrogel and DOX/FOK (right) peptide hydrogel at pH 7.4 after 6 months. Circle sweep of (B) FOK and (C) DOX/FOK hydrogels after 6 months.

technology. Fig. 7A shows that the fluorescence intensity of the free DiR group rapidly decreased over time, while the DiR/FOK group still exhibited significant and concentrated fluorescence 96 hours after administration, indicating that the FOX hydrogel carrier effectively prolonged the drug's duration of action in the body, enhancing its efficacy. Fig. 7B further revealed that, 96

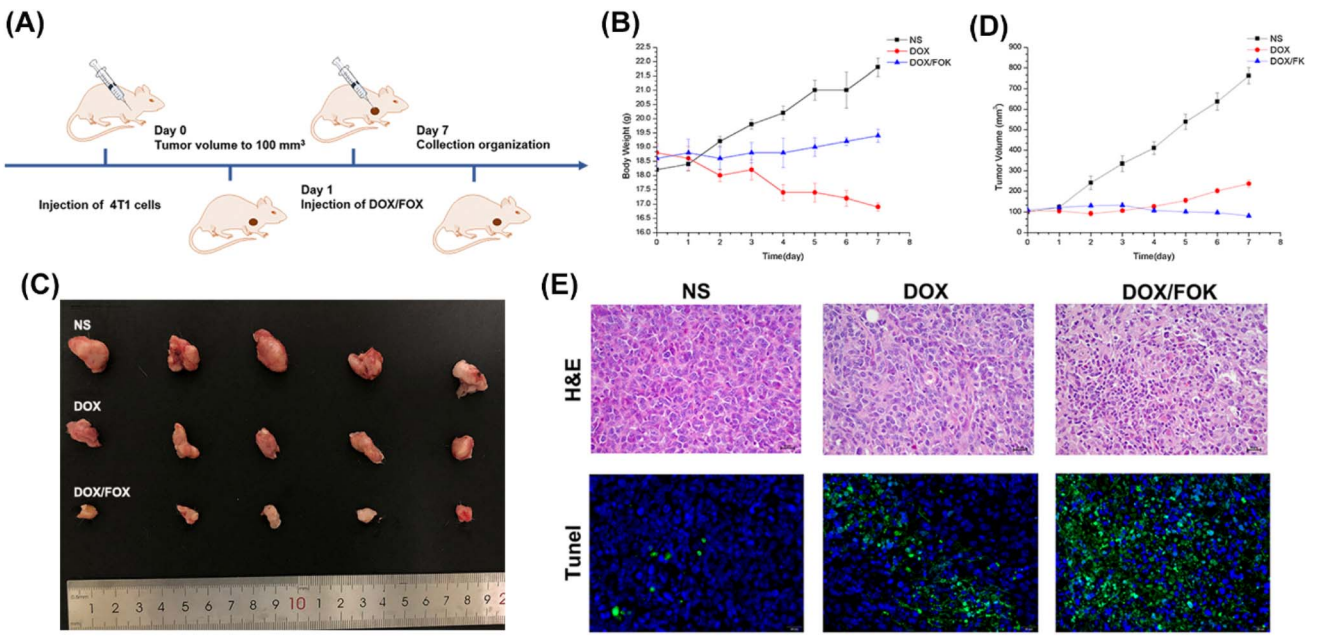

Fig. 6 (A) Schematic diagram of AuNRs-PU elimination bacterial biofilm. (B) The body weight change curve of mice after administration. (C) Images of the tumors harvested from the NS group, the DOX group and the DOX/FOK group mice 7 days after administration. (D) The tumor volume change curve of mice after administration. (E) H&E staining and Tunel assay images of tumor tissues dissected after treatment.

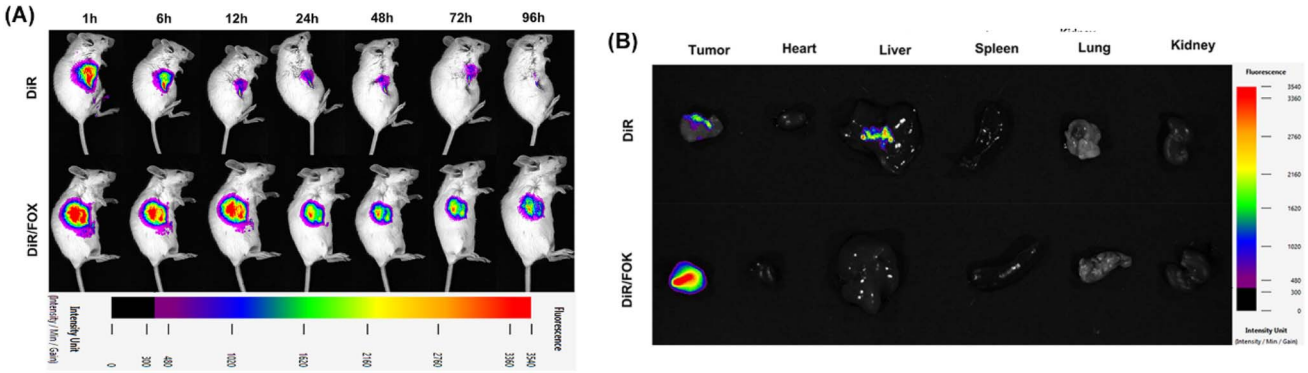

Fig. 7 (A) *In vivo* fluorescence images of tumor-bearing mice over time after administration of DiR and DiR/FOK. (B) *Ex vivo* fluorescence imaging of tumor, heart, liver, spleen, lung, and kidney dissected from tumor-bearing mice.

hours after administration, the DiR/FOK group showed DiR fluorescence still concentrated at the tumor site, with no significant fluorescence signals in other organs; in contrast, the free DiR group exhibited widespread fluorescence distribution (especially in the liver region), consistent with the *in vivo* imaging results, confirming that DOX/FOX hydrogel can concentrate drugs at the tumor site, prolong drug retention, significantly reduce systemic toxicity of chemotherapy drugs, and demonstrate the superiority of FOX as a drug carrier.

3.9 *In vitro* and *in vivo* biocompatibility

The cytotoxicity of blank hydrogels was determined using the CCK-8 method. As shown in Fig. 8A, even at a high FOK concentration of up to 400 μg mL^{-1}, the cell viability of 4T1 cells remained above 95%, strongly demonstrating the excellent biocompatibility of the hydrogel *in vitro*, making it suitable as a delivery platform for anti-tumor drugs. Furthermore, by comparing the proliferation inhibition effects of free DOX and DOX/FOK hydrogels on 4T1 cells under different pH conditions (Fig. 8B), it was found that both exhibited concentration-dependent inhibition, but when the DOX concentration exceeded 10 μg mL^{-1}, the enhancement effect tended to saturate. DOX/FOK showed stronger cytotoxicity at pH 6.0, attributed to the acidic-triggered release mechanism. IC_{50} value analysis (Table S6†) revealed that the IC_{50} value of DOX/FOK was higher than that of free DOX, indicating lower cytotoxicity, attributed to the sustained-release characteristics of the hydrogel, releasing only about 58.62% of the drug within 48 hours,

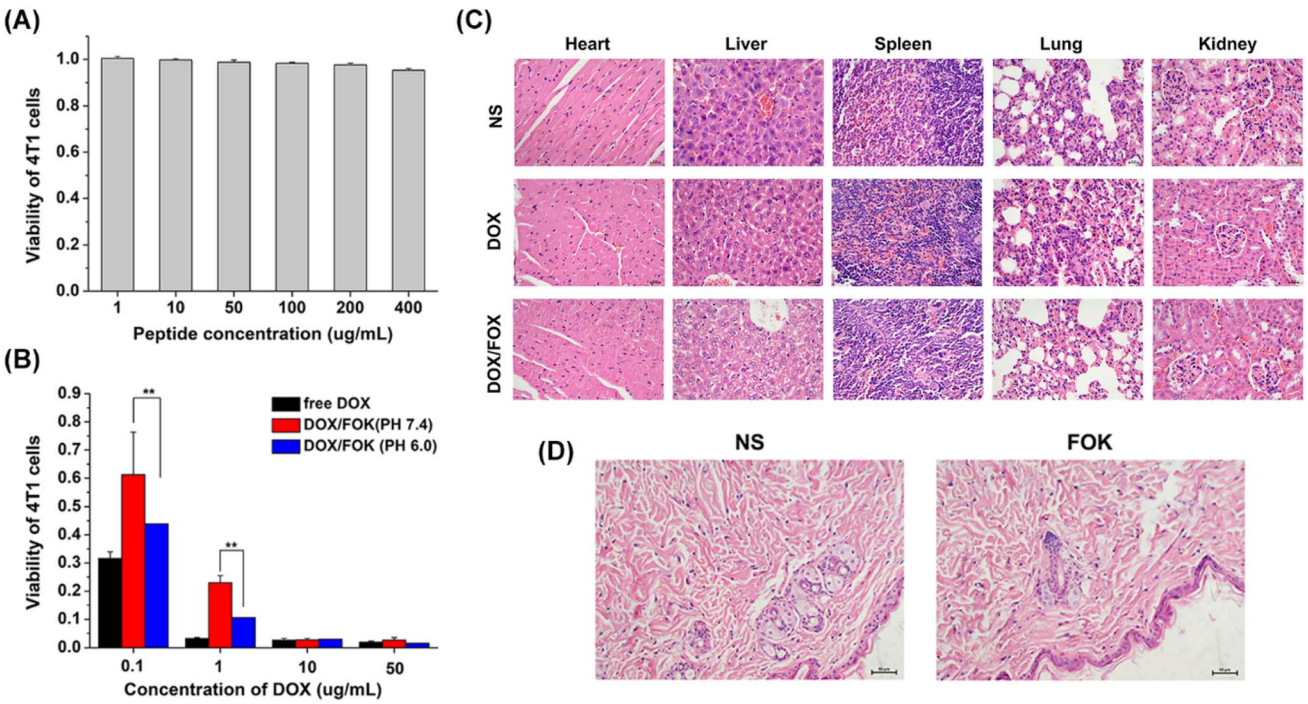

Fig. 8 (A) Cell viability of 4T1 cells co-incubated with FOK peptide hydrogel ($n = 6$). (B) Cell viability of 4T1 cells co-incubated with free DOX or DOX-loaded hydrogel ($n = 5$). (C) H&E staining images of heart, liver, spleen, lung and kidney dissected after treatment. (D) H&E-based immunohistochemical images of skin tissue.

thereby reducing drug toxicity and prolonging the duration of action.

To comprehensively evaluate the *in vivo* safety of DOX/FOK hydrogels, major organs of mice after treatment were subjected to H&E staining analysis (Fig. 8C). Compared to the significant necrosis of heart and liver cells in the DOX group, the organ cell morphology of the DOX/FOK and NS groups remained intact, with normal structure and no apparent damage, indicating a certain level of biological safety *in vivo*. Additionally, tissue H&E staining after subcutaneous injection of blank FOK hydrogels (Fig. 8D) showed normal cell morphology, tight tissue texture, and no signs of inflammatory cell infiltration or local bleeding, further demonstrating the good *in vivo* biocompatibility of FOK hydrogels.

4. Conclusions

This study aims to address the challenges faced by anti-tumor drugs such as limited bioavailability, short half-life, and poor selectivity. A pH-responsive peptide hydrogel based on hemopressin was innovatively designed and synthesized as a drug carrier. By systematically evaluating the gelation, pH responsiveness, and drug loading performance of four self-assembled peptides (POH, POK, FOH, FOK), FOX was selected as the optimal carrier, with the best concentration ratio of FOX 20 mg mL^{-1} and DOX 1 mg mL^{-1}. FOX hydrogel exhibited excellent pH sensitivity, forming a stable gel under physiological conditions (pH 7.4) and rapidly transforming into a highly mobile viscous liquid under acidic conditions in the tumor microenvironment (pH 6.0), indicating its huge potential as a drug carrier for anti-tumor drugs. Meanwhile, FOK showed extraordinary mechanical strength and stability, ensuring long-term drug storage and effective injection. *In vitro* and *in vivo* experiments confirmed that DOX/FOX hydrogel not only achieved precise controlled release of DOX and reduced toxicity, but also significantly enhanced anti-tumor efficacy. Studies on the distribution in mice showed that the hydrogel could precisely concentrate drugs at the tumor site, prolong drug retention time, and greatly reduce systemic toxicity. CCK-8 tests and *in vivo* animal models further confirmed the excellent biocompatibility of FOK hydrogel. In conclusion, the injectable pH-responsive hydrogel FOX developed in this study has enhanced the precise delivery, retention time, and local concentration of drugs through localized administration and intelligent responsiveness to the tumor microenvironment, effectively enhancing anti-cancer efficacy and reducing systemic side effects, providing an efficient and safe new approach for anti-cancer drug delivery strategies.

Data availability

Data will be available upon request to corresponding author.

Conflicts of interest

There are no conflicts to declare.

Acknowledgements

The Scientific Research Project of Nantong Health Commission (MSZ2022015).

References

1 C. Wu, M. Li, H. Meng, Y. Liu, W. Niu, Y. Zhou, R. Zhao, Y. Duan, Z. Zeng, X. Li, G. Li, W. Xiong and M. Zhou, Analysis of status and countermeasures of cancer incidence and mortality in China, *Sci. China: Life Sci.*, 2019, **62**(5), 640–647.

2 M. D. M. Sáez-Freire, A. Blanco-Gómez, S. Castillo-Lluva, A. Gómez-Vecino, J. M. Galvis-Jiménez, C. Martín-Seisdedos, M. Isidoro-García, L. Hontecillas-Prieto, M. B. García-Cenador, F. J. García-Criado, M. C. Patino-Alonso, P. Galindo-Villardón, J. H. Mao, C. Prieto, A. Castellanos-Martín, L. Kaderali and J. Pérez-Losada, The biological age linked to oxidative stress modifies breast cancer aggressiveness, *Free Radical Biol. Med.*, 2018, **120**, 133–146.

3 E. Pérez-Herrero and A. Fernández-Medarde, Advanced targeted therapies in cancer: Drug nanocarriers, the future of chemotherapy, *Eur. J. Pharm. Biopharm.*, 2015, **93**, 52–79.

4 G. Wei, Y. Wang, G. Yang, Y. Wang and R. Ju, Recent progress in nanomedicine for enhanced cancer chemotherapy, *Theranostics*, 2021, **11**(13), 6370–6392.

5 Z. Yu, Z. Xiao, X. Shuai and J. Tian, Local delivery of sunitinib and Ce6 *via* redox-responsive zwitterionic hydrogels effectively prevents osteosarcoma recurrence, *J. Mater. Chem. B*, 2020, **8**(30), 6418–6428.

6 M. Baxter-Holland and C. R. Dass, Doxorubicin, mesenchymal stem cell toxicity and antitumour activity: implications for clinical use, *J. Pharm. Pharmacol.*, 2018, **70**(3), 320–327.

7 N. Pilco-Ferreto and G. M. Calaf, Influence of doxorubicin on apoptosis and oxidative stress in breast cancer cell lines, *Int. J. Oncol.*, 2016, **49**(2), 753–762.

8 M. Songbo, H. Lang, C. Xinyong, X. Bin, Z. Ping and S. Liang, Oxidative stress injury in doxorubicin-induced cardiotoxicity, *Toxicol. Lett.*, 2019, **307**, 41–48.

9 P. S. Rawat, A. Jaiswal, A. Khurana, J. S. Bhatti and U. Navik, Doxorubicin-induced cardiotoxicity: An update on the molecular mechanism and novel therapeutic strategies for effective management, *Biomed. Pharmacother.*, 2021, **139**, 111708.

10 A. Hosseini and A. Sahebkar, Reversal of Doxorubicin-induced Cardiotoxicity by Using Phytotherapy: A Review, *J. Pharmacopuncture*, 2017, **20**(4), 243–256.

11 C. Hu, X. Zhang, P. Song, Y. P. Yuan, C. Y. Kong, H. M. Wu, S. C. Xu, Z. G. Ma and Q. Z. Tang, Meteorin-like protein attenuates doxorubicin-induced cardiotoxicity *via* activating cAMP/PKA/SIRT1 pathway, *Redox Biol.*, 2020, **37**, 101747.

12 A. Domiński, T. Konieczny, M. Godzierz, M. Musioł, H. Janeczek, A. Foryś, M. Domińska, G. Pastuch-Gawołek, T. Piotrowski and P. Kurcok, Co-Delivery of 8-

Hydroxyquinoline Glycoconjugates and Doxorubicin by Supramolecular Hydrogel Based on α-Cyclodextrin and pH-Responsive Micelles for Enhanced Tumor Treatment, *Pharmaceutics*, 2022, **14**(11), 2490.

13 W. Chen, K. Shi, J. Liu, P. Yang, R. Han, M. Pan, L. Yuan, C. Fang, Y. Yu and Z. Qian, Sustained co-delivery of 5-fluorouracil and cis-platinum *via* biodegradable thermosensitive hydrogel for intraoperative synergistic combination chemotherapy of gastric cancer, *Bioact. Mater.*, 2023, **23**, 1–15.

14 W. Ahn, J. H. Lee, S. R. Kim, J. Lee and E. J. Lee, Designed protein- and peptide-based hydrogels for biomedical sciences, *J. Mater. Chem. B*, 2021, **9**(8), 1919–1940.

15 Z. Yu, Z. Cai, Q. Chen, M. Liu, L. Ye, J. Ren, W. Liao and S. Liu, Engineering β-sheet peptide assemblies for biomedical applications, *Biomater. Sci.*, 2016, **4**(3), 365–374.

16 P. Worthington, S. Langhans and D. Pochan, β-hairpin peptide hydrogels for package delivery, *Adv. Drug Deliv. Rev.*, 2017, **110–111**, 127–136.

17 L. A. Castillo-Díaz, J. A. Ruiz-Pacheco, M. A. Elsawy, J. E. Reyes-Martínez and A. I. Enríquez-Rodríguez, Self-Assembling Peptides as an Emerging Platform for the Treatment of Metabolic Syndrome, *Int. J. Nanomed.*, 2020, **15**, 10349–10370.

18 M. Amit, S. Yuran, E. Gazit, M. Reches and N. Ashkenasy, Tailor-Made Functional Peptide Self-Assembling Nanostructures, *Adv. Mater.*, 2018, **30**(41), e1707083.

19 Z. Lin, J. Ding, X. Chen and C. He, pH- and Temperature-responsive Hydrogels Based on Tertiary Amine-modified Polypeptides for Stimuli-responsive Drug Delivery, *Chem. Asian J.*, 2023, **18**(8), e202300021.

20 Y. Zhou, Z. Chen, D. Zhao, D. Li, C. He and X. Chen, A pH-Triggered Self-Unpacking Capsule Containing Zwitterionic Hydrogel-Coated MOF Nanoparticles for Efficient Oral Exendin-4 Delivery, *Adv. Mater.*, 2021, **33**(32), e2102044.

21 S. Chen, L. Rong, Q. Lei, P. X. Cao, S. Y. Qin, D. W. Zheng, H. Z. Jia, J. Y. Zhu, S. X. Cheng, R. X. Zhuo and X. Z. Zhang, A surface charge-switchable and folate modified system for co-delivery of proapoptosis peptide and p53 plasmid in cancer therapy, *Biomaterials*, 2016, **77**, 149–163.

22 J. Gao, J. Zhan and Z. Yang, Enzyme-Instructed Self-Assembly (EISA) and Hydrogelation of Peptides, *Adv. Mater.*, 2020, **32**(3), e1805798.

23 F. Andrade, M. M. Roca-Melendres, E. F. Durán-Lara, D. Rafael and S. Schwartz Jr, Stimuli-Responsive Hydrogels for Cancer Treatment: The Role of pH, Light, Ionic Strength and Magnetic Field, *Cancers*, 2021, **13**(5), 1164.

24 Z. Sun, C. Song, C. Wang, Y. Hu and J. Wu, Hydrogel-Based Controlled Drug Delivery for Cancer Treatment: A Review, *Mol. Pharm.*, 2020, **17**(2), 373–391.

25 J. Xu, A. Gulzar, D. Yang, S. Gai, F. He and P. Yang, Tumor self-responsive upconversion nanomedicines for theranostic applications, *Nanoscale*, 2019, **11**(38), 17535–17556.

26 Y. Liu, Y. Ran, Y. Ge, F. Raza, S. Li, H. Zafar, Y. Wu, A. C. Paiva-Santos, C. Yu, M. Sun, Y. Zhu and F. Li, pH-Sensitive Peptide Hydrogels as a Combination Drug Delivery System for Cancer Treatment, *Pharmaceutics*, 2022, **14**(3), 652.

27 P. Mondal, I. Chakraborty and K. Chatterjee, Injectable Adhesive Hydrogels for Soft tissue Reconstruction: A Materials Chemistry Perspective, *Chem. Rec.*, 2022, **22**(11), e202200155.

28 P. Mondal and K. Chatterjee, Injectable and self-healing double network polysaccharide hydrogel as a minimally-invasive delivery platform, *Carbohydr. Polym.*, 2022, **291**, 119585.

29 S. Yu, C. He and X. Chen, Injectable Hydrogels as Unique Platforms for Local Chemotherapeutics-Based Combination Antitumor Therapy, *Macromol. Biosci.*, 2018, **18**(12), e1800240.

30 I. Gomes, C. S. Dale, K. Casten, M. A. Geigner, F. C. Gozzo, E. S. Ferro, A. S. Heimann and L. A. Devi, Hemoglobin-derived peptides as novel type of bioactive signaling molecules, *AAPS J.*, 2010, **12**(4), 658–669.

31 A. S. Heimann, C. S. Dale, F. S. Guimarães, R. A. M. Reis, A. Navon, M. A. Shmuelov, V. Rioli, I. Gomes, L. L. Devi and E. S. Ferro, Hemopressin as a breakthrough for the cannabinoid field, *Neuropharmacology*, 2021, **183**, 108406.

32 H. M. Dao, J. Chen, B. S. Tucker, V. Thomas, H. W. Jun, X. C. Li and S. Jo, Hemopressin-Based pH-Sensitive Hydrogel: A Potential Bioactive Platform for Drug Delivery, *ACS Biomater. Sci. Eng.*, 2018, **4**(7), 2435–2442.

33 F. Wei, L. Zhao and Y. Jing, Signaling molecules targeting cannabinoid receptors: Hemopressin and related peptides, *Neuropeptides*, 2020, **79**, 101998.

34 Y. Liu, Y. Liu, X. Sun, Y. Wang, C. Du and J. Bai, Morphologically transformable peptide nanocarriers coloaded with doxorubicin and curcumin inhibit the growth and metastasis of hepatocellular carcinoma, *Mater. Today Bio*, 2024, **24**, 100903.

35 J. Ma, H. Yang, X. Tian, F. Meng, X. Zhai, A. Li, C. Li, M. Wang, G. Wang, C. Lu and J. Bai, Matrix metalloproteinase 2-responsive dual-drug-loaded self-assembling peptides suppress tumor growth and enhance breast cancer therapy, *Bioeng. Transl. Med.*, 2024, e10702.

36 M. A. Elsawy, J. K. Wychowaniec, L. A. Castillo Díaz, A. M. Smith, A. F. Miller and A. Saiani, Controlling Doxorubicin Release from a Peptide Hydrogel through Fine-Tuning of Drug-Peptide Fiber Interactions, *Biomacromolecules*, 2022, **23**(6), 2624–2634.

37 Y. Yuan, Q. Zhang, S. Lin and J. Li, Water: The soul of hydrogels, *Prog. Mater. Sci.*, 2025, **148**, 101378.

38 S. K. Mandal, T. Kar and P. K. Das, Pristine carbon-nanotube-included supramolecular hydrogels with tunable viscoelastic properties, *Chemistry*, 2013, **19**(37), 12486–12496.

39 D. Zaguri, M. R. Zimmermann, G. Meisl, A. Levin, S. Rencus-Lazar, T. P. J. Knowles and E. Gazit, Kinetic and Thermodynamic Driving Factors in the Assembly of Phenylalanine-Based Modules, *ACS Nano*, 2021, **15**(11), 18305–18311.